Palm-top size megawatt peak power ultraviolet microlaser

Rakesh Bhandari
Takunori Taira

SPIE

Palm-top size megawatt peak power ultraviolet microlaser

Rakesh Bhandari
Takunori Taira
Laser Research Center
Institute for Molecular Science
38 Nishigonaka, Myodaiji
Okazaki 444-8585, Japan
E-mail: bhandari@ims.ac.jp

Abstract. The development of a very compact, highly efficient, megawatt peak power, subnanosecond pulse width, 266 nm ultraviolet (UV) microlaser is reported. It contains a specially designed passively Q-switched $Nd\!:\!YAG/Cr^{4+}\!:\!YAG$ microchip laser whose high output peak power of 13 MW enables an efficient wavelength conversion without using any optics before the nonlinear crystals. The subnanosecond pulse width region, which delivers high peak power even at moderate pulse energy, is very useful for an efficient wavelength conversion. We achieve 73% second harmonic generation efficiency using a LiB_3O_5 (lithium triborate) crystal and 45% fourth harmonic generation efficiency using a $\beta - BaB_2O_4$ (β-barium borate) crystal. As a result, we obtain 650 μJ, 4.3 MW peak power, 150 ps, and 100 Hz pulse output at 266 nm. We use an original design for the nonlinear crystal holders to reduce the size of the micro-laser. This palm-top size 266 nm UV microlaser will be useful for many applications, such as materials microprocessing, pulsed laser deposition, UV laser induced breakdown spectroscopy, and photoionization. © The Authors. Published by SPIE under a Creative Commons Attribution 3.0 Unported License. Distribution or reproduction of this work in whole or in part requires full attribution of the original publication, including its DOI. [DOI: 10.1117/1.OE.52.7.076102]

1 Introduction

Giant pulse ultraviolet (UV) lasers are needed for several industrial and scientific applications, such as materials microprocessing, fast prototyping, pulsed laser deposition, and photoionization. However, the large size and high cost of high energy pulsed UV lasers have drastically limited their use. Further, UV lasers, such as excimer lasers, are difficult to maintain.

Microchip lasers provide pulsed power in a compact, low-cost configuration. This can be effectively used for wavelength conversion, as reported earlier by Zayhowski et al.[1,2] However, the peak power of the microchip lasers used was in the kilowatt range and so the wavelength conversion efficiency achieved was modest. We have been working on the development of very compact, giant-pulse (>1 MW peak power) $Nd\!:\!YAG/Cr^{4+}\!:\!YAG$ microchip lasers using quasi-continuous-wave (QCW) pumping for several applications.[3,4] We have used these lasers to develop a laser ignition module that can be used in automobiles to replace spark plugs.[5,6] These lasers have a high peak power (>6 MW). However, the output of these lasers is not stable, linearly polarized. Hence, they cannot be used, as is, for an efficient wavelength conversion. We proposed the use of [110]-cut $Cr^{4+}\!:\!YAG$, instead of the normally used [100]-cut $Cr^{4+}\!:\!YAG$, to achieve a stable, linearly polarized output.[7] With this approach, we have obtained several megawatt peak power, linearly polarized output with a passively Q-switched $Nd\!:\!YAG/Cr^{4+}\!:\!YAG$ microchip laser. Using this microchip laser output, we have achieved 85% second harmonic generation (SHG) efficiency using a type I lithium triborate (LBO) crystal,[8] and 61% fourth harmonic generation (FHG) efficiency using a fluxless-grown barium borate (BBO) crystal.[9] These results were obtained under optimum conditions using focusing optics to input the laser beam into the nonlinear crystals.

The focusing optics between the laser and the nonlinear crystals and the rotational stages required to orient the nonlinear crystals limit the advantage that can be obtained by the high fundamental peak power in reducing the size of the laser. In this paper, we report the development of a palm-top size UV microlaser whose compactness is increased by eliminating any focusing optics between the laser source and the nonlinear crystals and by not using any commercial rotational stages. At the heart of this system is a passively Q-switched $Nd\!:\!YAG/Cr^{4+}\!:\!YAG$ microchip laser developed by us which provides a peak power of 13 MW. Commercially available LBO and BBO crystals are used for SHG and FHG, respectively. The high peak power of the fundamental beam enables us to perform wavelength conversion without using any optics before the nonlinear crystals. A specially designed housing for the nonlinear crystals allows three-axis orientation to achieve high conversion efficiency even in the critical phase matching (CPM) regime.

As a result, we obtain 650 μJ, 4.3 MW peak power, 150 ps, and 100 Hz pulses at 266 nm in a very compact laser structure. To our knowledge, this is the first report of a palm-top size, MW peak power UV laser.

2 Laser Structure

A schematic of the microlaser configuration is given in Fig. 1.

The microchip laser uses a 4-mm thick 1.1 at.% [111]-cut $Nd\!:\!YAG$ crystal (Scientific Materials Corp., Bozeman, Montana) which was pumped in the QCW regime by a fiber-coupled 120 W and 808 nm laser diode (600 μm core diameter, 0.22 NA, JOLD-120-QPXF-2P of Jenoptik) at
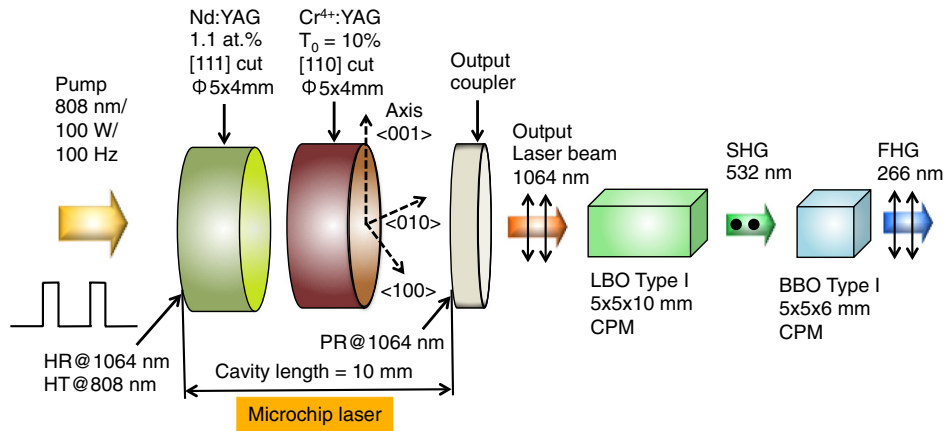
Fig. 1 Laser configuration with no intervening optics before nonlinear crystals.

100 Hz. A 10% initial transmission [110]-cut Cr^{4+}:YAG crystal (Scientific Materials Corp.) was used for passive Q-switching. A flat coupler with a transmission of 50% was used at the output. The cavity length was 10 mm. A thermoelectric cooler was used to maintain the Nd:YAG and Cr^{4+}:YAG crystal temperature at 24°C. The laser structure had dimensions of $60 \times 52 \times 61$ mm^3 and was air cooled.[8,9]

The microchip laser is similar to that used by us earlier,[8,9] except that we have used a 10% initial transmission Cr^{4+}:YAG, instead of the 30% initial transmission used earlier, in order to increase the lasing threshold, and consequently, the population inversion ratio. This reduces the pulse width and increases the peak power of the microchip laser. We did this to achieve high laser intensity without the need for focusing the laser beam.

SHG was obtained by using a 5×5 mm^2 cross-section, 10-mm long type I LBO crystal ($\theta = 90$ deg, $\varphi = 11.4$ deg). The crystal was dual-band antireflection coated at 532 and 1064 nm. We chose LBO for SHG due to its high-enough damage threshold and a relatively large angular acceptance bandwidth that permits efficient SHG even with a multimode laser beam. We performed SHG in the CPM regime since any crystal temperature control mechanism would increase the overall size, and so diminish the size advantage offered by compact microchip lasers. The LBO crystal was placed in a specially designed holder. It consists of a brass sphere with a groove cut at the center to place the crystal. The sphere can be freely rotated on a hemispherical base to adjust the three-axis angular orientation of the crystal with respect to the laser beam. This mechanism, used instead of a three-axis rotation stage, reduced the overall size of the microlaser. There was no intervening optics between the microchip laser and the LBO crystal.

For FHG, we used a 5×5 mm^2 cross-section 6-mm long type I BBO crystal ($\theta = 47.7$ deg, $\varphi = 0$ deg), in the CPM regime. The crystal was dual-band antireflection coated at 532 and 266 nm. Again, no intervening optics was used between the LBO and BBO crystals. A BBO crystal was used for FHG because of its ease of handling, as it is less hygroscopic compared to $CsLiB_6O_{10}$ (CLBO). The BBO crystal was also placed in a groove cut in a brass sphere that could be freely rotated on a hemispherical base to adjust the three-axis angular orientation of the crystal.

The photographs of two prototypes of the microlaser are shown in Fig. 2. The microlaser, shown in Fig. 2(a), has
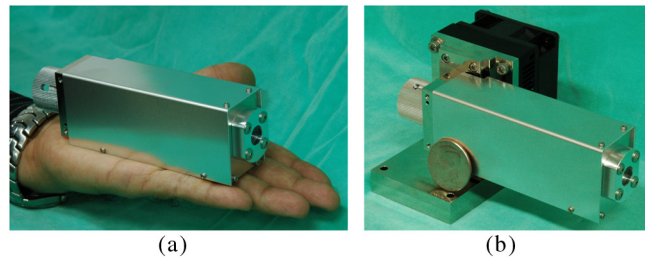

Fig. 2 Photograph of microlaser prototype without cooling (a) and with thermoelectric cooling (b).

dimensions of $150 \times 35 \times 45$ mm^3. Along with a thermoelectric cooler and a cooling fan, which allow operation under ambient temperature fluctuations, the dimensions are $155 \times 95 \times 60$ mm^3. Optimizing the component placement and packaging can further reduce the dimensions.

3 Experimental Results

3.1 Fundamental Laser Characteristics

Using the microchip laser structure described above, we obtained a stable, linearly polarized output of 3 mJ pulse energy, 230 ps pulse width, and 100 Hz repetition rate at 1064 nm for 100 W, 275 μs width 100 Hz QCW pumping. This results in a peak power of 13 MW. The polarization of the output beam was stable, with an extinction ratio of better than 1:100, due to the use of [110]-cut Cr^{4+}:YAG for passive Q-switching. The output pulse temporal profile is shown in Fig. 3. We did not notice any multiple pulses due to the use of 10% initial transmission Cr^{4+}:YAG, which results in a high lasing threshold. The output power stability was better than 1% for more than 8 h of continuous measurement.

3.2 SHG Characteristics

SHG was performed using a commercial, type I LBO crystal in the CPM regime at room temperature (22°C). The beam diameter at the LBO input face was ~0.8 mm. The LBO crystal holder was rotated along the three axes to maximize the output at 532 nm. By proper angle tuning, we could obtain 1.7 mJ pulse energy and 177 ps pulse width output at 532 nm. This gives a peak power of 9.5 MW and a conversion efficiency of 73%. Although this conversion
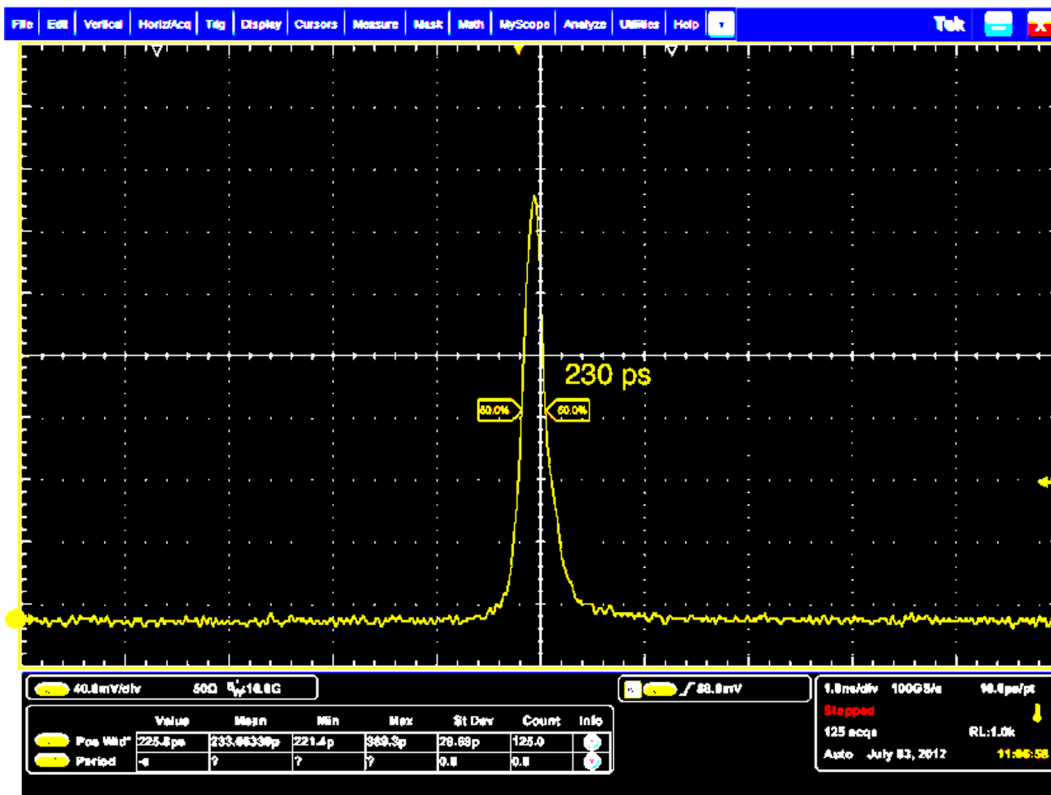
Fig. 3 Temporal profile of the fundamental laser output having a pulse width of 230 ps, measured using Tektronix DPO71604C oscilloscope and EOT ET-3500 detector.

efficiency is lower than the maximum conversion efficiency of 85% obtained by us under optimum conditions when optics is used to launch the laser beam into the LBO crystal,[8] it is still high due to the high input peak power. The temporal beam profile at 532 nm is shown in Fig. 4.

3.3 *FHG Characteristics*

For FHG, we used a commercial, type I BBO crystal in the CPM regime at room temperature (22°C). The BBO crystal holder was rotated along the three axes to maximize the output at 266 nm, as measured after two dichroic mirrors to separate the fundamental and 532 nm from the 266 nm beam. It was found necessary to finely retune the LBO crystal in order to maximize the 266-nm output. We believe that this is due to the fact that we are not optimizing the conditions at each stage.

We obtained 650 μJ pulse energy and 150 ps pulse width output at 266 nm. This gives a peak power of 4.3 MW and a conversion efficiency of 45.3%. The FHG conversion efficiency is lower than the 60% that was obtained under optimum focusing conditions using a fluxless-grown BBO crystal.[9] However, the microlaser can be made more compact and stable by eliminating the optics between the LBO and BBO crystals. The overall conversion efficiency from 1064 to 266 nm is ∼33%, without the use of any intervening optics.

The temporal beam profile and the spatial beam profile at 266 nm are shown in Fig. 5(a) and 5(b), respectively. The M^2 of the output 266-m beam was measured by the knife-edge method and was calculated to be 2.4 and 2.6 in the vertical and horizontal directions, respectively. The measurements are shown in Fig. 6.

4 Discussion

The very good results achieved here for wavelength conversion are largely due to the use of the subnanosecond "pulse gap" region.[10] Actively Q-switched nanosecond lasers provide pulse widths ranging from a few nanoseconds to hundreds of nanoseconds. On the other hand, mode-locked lasers provide pulse widths from a few femtoseconds to less than 100 ps. Hence, if only these two types of lasers are used, there is a pulse gap between 100 ps and 1 ns, which is not easily accessible. This pulse gap region can be accessed by the use of passively Q-switched lasers. This pulse width region can enable peak power of a few megawatts even for a moderate pulse energy of a few millijoules and can be effectively used for high-efficiency wavelength conversion.

To understand how the pulse gap region is suitable for high-efficiency wavelength conversion, consider the following relation for wavelength conversion efficiency, η:

$$\eta \propto \tanh^2\left[L\left(\frac{P_\omega}{A}\right)^{1/2} \right], \tag{1}$$

where L is the length of the nonlinear crystal, P_ω is the laser input power, and A is the effective input beam area. When a nanosecond laser is used for wavelength conversion, since the peak power of a nanosecond laser is not very high, we are required to focus the laser beam in order to increase the P_ω/A term in Eq. (1), to increase the conversion efficiency. However, due to the walk-off of the nonlinear crystal, this limits the interaction length in the crystal and so limits the conversion efficiency.
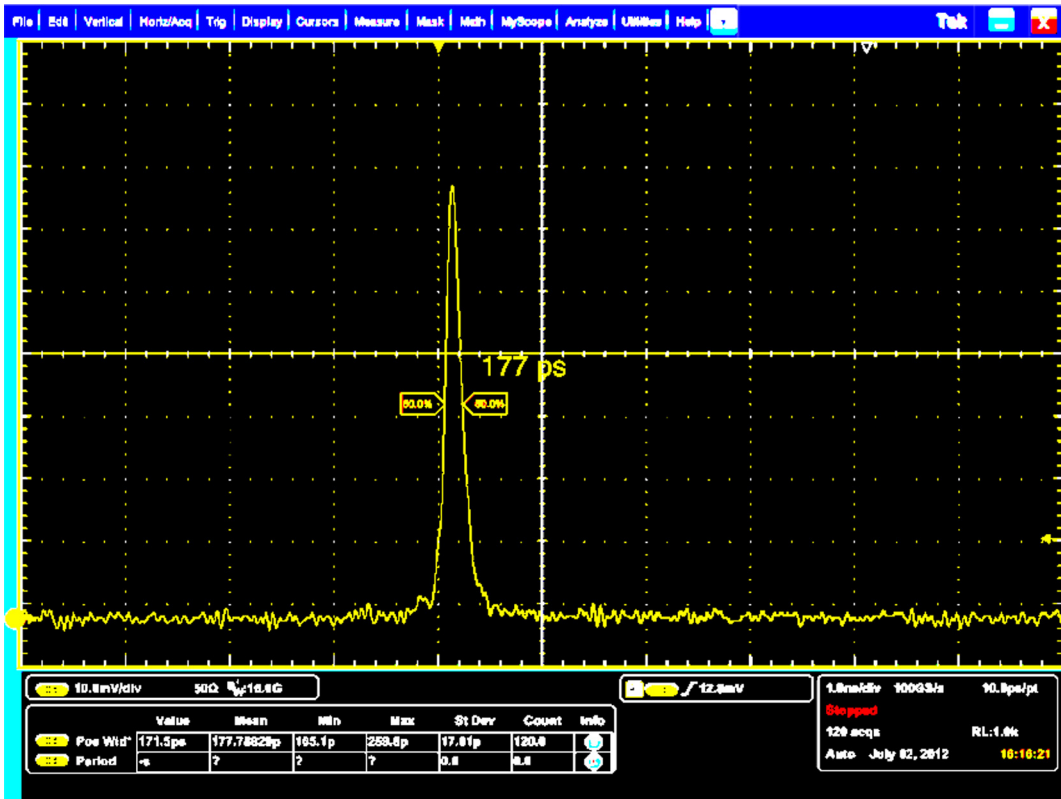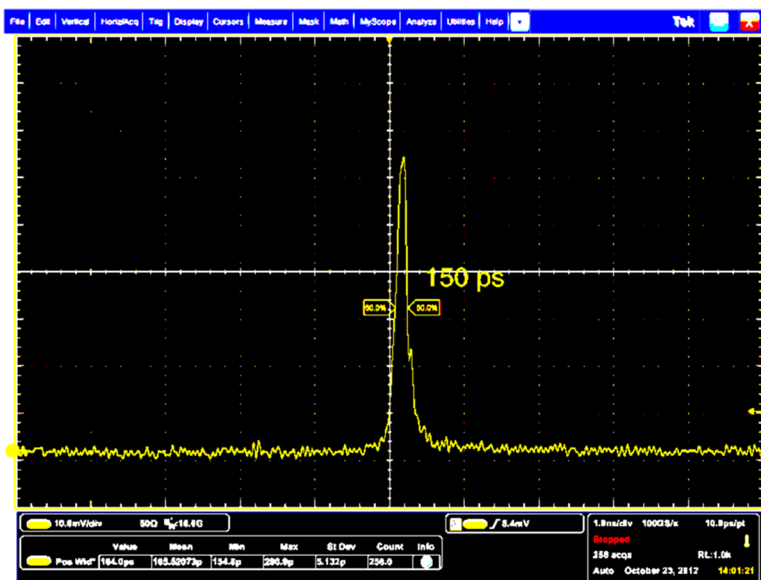
Fig. 4 Temporal profile of SHG output having a pulse width of 177 ps, measured using Tektronix DPO71604C oscilloscope and EOT ET-4000 detector.

On the other hand, when a femtosecond laser is used for wavelength conversion, since the peak power of the femtosecond laser is high, we need not focus the laser beam. However, the wide spectrum of a femtosecond laser beam limits the length of the nonlinear crystal used. Otherwise, the input laser pulse gets broadened due to group velocity mismatch. Normally, for femtosecond lasers, a nonlinear crystal of a few hundred-microns thickness is used. This makes the term L in Eq. (1) small, and so the conversion efficiency is small.

For a laser having a pulse width in the pulse gap region (100 ps to 1 ns), the peak power is high and the spectrum width is still small. Hence, it is possible to use a long nonlinear crystal without, or with minimal, focusing of the laser

(a)
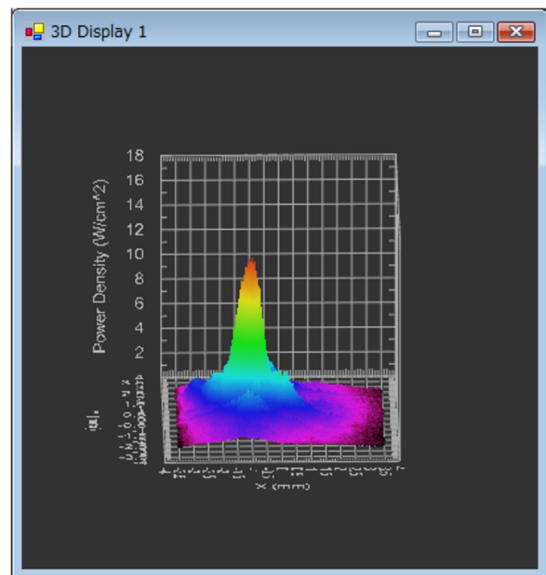
(b)

Fig. 5 (a) Temporal profile of FHG output having a pulse width of 177 ps, measured using Tektronix DPO71604C oscilloscope and Alphalas UPD-50-UD detector. (b) Beam profile of FHG pulse.
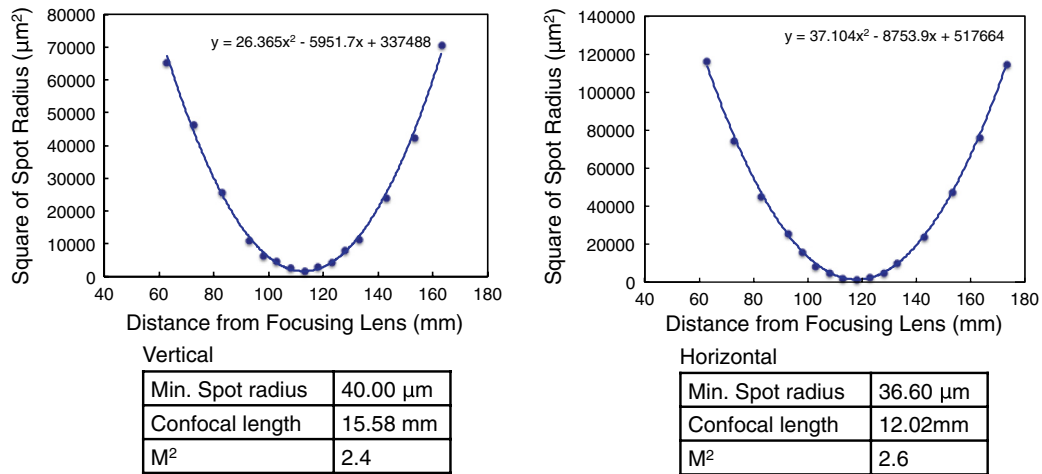
Vertical	
Min. Spot radius	40.00 μm
Confocal length	15.58 mm
M^2	2.4

Horizontal	
Min. Spot radius	36.60 μm
Confocal length	12.02mm
M^2	2.6

Fig. 6 M^2 measurement results for the output FHG beam.

beam. In other words, both the P_ω/A and L terms in Eq. (1) can be made large, and so high conversion efficiency can be achieved.

Further, there is another advantage of not focusing the laser beam. Traditionally, pulsed UV lasers have suffered from a drawback that the BBO crystal used for the FHG gets damaged over a short period of time because the second harmonic beam is required to be focused tightly into the BBO crystal to achieve reasonably acceptable conversion efficiency. This affects the BBO surface coating and also leads to two-photon absorption in the BBO crystal. To counter this, the BBO crystal is moved/rotated at a regular time interval to change the position of the incident laser beam.

We have been able to eliminate the need for laser beam focusing by effectively using the subnanosecond pulse-gap region, as explained above. Consequently, we have avoided damage to the BBO crystal and have eliminated the need to periodically move it. The developed prototype has been in use for several months without any degradation of its output.

We would also like to mention that the microchip laser cavity was intentionally designed to achieve high pulse energy even though we had to sacrifice obtaining an ideal Gaussian beam. In fact, a Gaussian beam is not ideal for achieving maximum conversion efficiency since the wings of the pulse do not contribute to frequency conversion.[8,9]

5 Conclusion

We have designed and demonstrated a palm-top size UV microlaser that provides 650 μJ, 4.3 MW peak power, 150 ps, and 100 Hz pulse output at 266 nm. We have achieved 73% SHG conversion efficiency using a LBO crystal and 45% FHG conversion efficiency using a BBO crystal, without using any optics before the nonlinear crystals. This gives 33% conversion efficiency from IR to UV in a very compact size laser.

This compact UV microlaser can be used for several applications, such as materials microprocessing, pulsed laser deposition, UV laser-induced breakdown spectroscopy, and photoionization. We expect this microlaser to significantly expand the applications of pulsed UV lasers.

References

1. J. J. Zayhowski et al., "Mid-and high-power passively Q-switched microchip lasers," in *Proc. Advanced Solid-State Lasers*, M. M. Fejer, H. Injeyan, and U. Keller, Eds., Vol. 26 of OSA Trends in Optics and Photonic Series, pp. 178–186, Optical Society of America, Washington, DC (1999).
2. J. J. Zayhowski, "Ultraviolet generation with passively Q-switched microchip lasers," *Opt. Lett.* **21**(8), 588–590 (1996).
3. H. Sakai, H. Kan, and T. Taira, ">1 MW peak power single-mode high brightness passively Q-switched Nd^{3+}:YAG microchip laser," *Opt. Express* **16**(24), 19891–19899 (2008).
4. S. Hayashi et al., "Tunability enhancement of a terahertz-wave parametric generator pumped by a microchip Nd:YAG laser," *Appl. Opt.* **48**(15), 2899–2902 (2009).
5. M. Tsunekane et al., "High peak power, passively Q-switched microlaser for ignition of engines," *IEEE J. Quantum Electron.* **46**(2), 277–284 (2010).
6. N. Pavel, M. Tsunekane, and T. Taira, "Composite, all-ceramics, high-peak power Nd:YAG/Cr^{4+}:YAG monolithic micro-laser with multiple-beam output for engine ignition," *Opt. Express* **19**(10), 9378–9384 (2011).
7. H. Sakai, H. Kan, and T. Taira, "Passive Q-switch laser device," U.S. Patent No. 7,664,148 B2 (February 16 2010).
8. R. Bhandari and T. Taira, ">6 MW output power at 532 nm from passively Q-switched Nd:YAG/Cr^{4+}:YAG microchip laser," *Opt. Express* **19**(20), 19135–19141 (2011).
9. R. Bhandari and T. Taira, ">3 MW peak power at 266 nm using Nd:YAG/Cr^{4+}:YAG microchip laser and fluxless-BBO," *Opt. Mater. Express* **2**(7), 914–919 (2012).
10. T. Taira, "Domain-controlled laser ceramics toward giant microphotonics," *Opt. Mater. Express* **1**(5), 1040–1050 (2011).

Rakesh Bhandari graduated from Indian Institute of Technology in electrical engineering in 1976 and obtained his ME and PhD degrees in optoelectronics from Toyohashi University of Technology, Japan, in 1985 and 2001, respectively. He has over 12 years of experience in the design and fabrication of lasers and their applications. He has worked extensively on fiber lasers, mode-locked lasers, and chirped pulse amplifiers. His recent interests include passively Q-switched microchip lasers and their use in nonlinear optics, materials microprocessing, laser-induced breakdown spectroscopy (LIBS), etc. He is currently a Research Fellow at National Institutes of Natural Sciences, Institute for Molecular Science (IMS), Okazaki, Japan.

Takunori Taira received his BE and ME degrees in electrical engineering from Fukui University, Fukui, Japan, in 1983 and 1985, respectively, and his PhD degree in communication engineering from Tohoku University, Sendai, Japan, in 1996. He is currently an associate professor with the National Institutes of Natural Sciences, Institute for Molecular Science (IMS), Okazaki, Japan, and an Invited Professor at Pierre and Marie Curie University (Paris VI), Paris, France, in 2006, and Université Joseph Fourier, France, in 2011. He received the "2004 Commendation" Award of the Ministry of Education, Culture, Sports, Science, and Technology of Japan, for scientific and technological research merits (Japan) in 2004, and "The 24th Kenjiro Sakurai Memorial Prize: Award of The Optoelectronic Industry and Technology Development Association (OITDA)" (Japan) in 2008. He is an OSA Fellow since 2010, an IEEE Senior Member since 2011, and an SPIE Fellow since 2012.